Histol Histopathol (2018) 33: 417-432

http://www.hh.um.es

Histology and Histopathology

From Cell Biology to Tissue Engineering

Review

Quantitative phase microscopy for evaluation of intestinal inflammation and wound healing utilizing label-free biophysical markers

Dominik Bettenworth[1]*, Arne Bokemeyer[1]*, Christopher Poremba[2], Nik Sheng Ding[3], Steffi Ketelhut[4], Philipp Lenz[1,5#] and Björn Kemper[4#]

[1]Department of Medicine B, University Hospital Muenster, Muenster, [2]Department of Pathology, Pathology Munich-North, Munich, Germany, [3]Department of Medicine, University of Melbourne, Melbourne, Vic, Australia, [4]Biomedical Technology Center, University of Muenster and [5]Institute of Palliative Care, University Hospital Muenster, Muenster, Germany

*: these authors contributed equally and share first authorship

#: these authors contributed equally and share last authorship

Summary. Inflammatory bowel diseases (IBD) are inflammatory disorders of the gastrointestinal tract characterized by a chronic relapsing disease course. As uncontrolled intestinal inflammation can result in severe disease complications, recent treatment targets of IBD evolved toward seeking the absence of mucosal and histological inflammation. However, this approach requires adequate histological evaluation of IBD disease activity. The diagnostic challenge of histological examination of intestinal inflammation is documented by the multitude of proposed histological scoring systems. In this context, we review quantitative phase imaging (QPI) techniques such as digital holographic microscopy (DHM) for characterizing intestinal inflammation. DHM determines optical path-length delays in a stain-free manner, thereby providing the tissue refractive index as a biophysical marker that directly correlates to tissue density. Recently, DHM has been successfully applied in cell biology, cancer cell research and infectious-induced cellular alterations. We summarized the capabilities of DHM and related QPI techniques to assess the severity of intestinal inflammation in experimental colitis as well as in colonic samples from human IBD patients. Moreover, we illustrate major advantages of DHM facilitated multimodal evaluation of epithelial wound healing processes as assessed by physical parameters like cell volume, density, thickness and dry mass *in vitro*. Furthermore, potential limitations of DHM and future utilities of QPI are discussed. In conclusion, DHM represents a promising, easy-to-use quantitative tool to provide accurate and objective assessment of intestinal inflammation and may pave the way towards automated label-free digital pathology and related *in vitro* cell culture analysis in future.

Key words: Inflammatory bowel disease, Histological healing, Digital holographic microscopy, Quanitative phase microscopy

Offprint requests to: Dr. Björn Kemper, PhD, Biomedical Technology Center, University of Muenster, Mendelstraße 17, D-48149 Muenster, Germany. e-mail: bkemper@uni-muenster.de

DOI: 10.14670/HH-11-937

Introduction

Inflammatory bowel disease (IBD), including Crohn's disease (CD) and ulcerative colitis (UC), are common inflammatory disorders of the gastrointestinal tract characterized by a chronic relapsing disease course (Baumgart and Sandborn, 2012; Ordas et al., 2012). Despite the fact that the therapeutic armamentarium available to clinicians has increased over recent years, a sustained maintenance of remission cannot be achieved in a significant number of IBD patients (Qiu et al., 2017). Furthermore, chronic, uncontrolled intestinal inflammation can lead to various disease complications requiring hospitalization and surgery, which is associated with a high economic disease burden (Park and Bass,

2011). Recently, treatment goals have evolved from symptom control to deep remission with histological healing reflected by the absence of inflammatory alterations in colonic biopsy samples. While several histological scoring systems have been proposed, nearly all of these scoring systems have not been fully validated and require appropriate expertise in the field of IBD pathology (Bryant et al., 2014; Mosli et al., 2014, 2017a,b). Thus, reliable, objective and easy-to-use diagnostic approaches to facilitate histological examination of colonic tissue samples are urgently needed. In this context, we discuss digital holographic microscopy (DHM) as an example of quantitative phase imaging (QPI) for label-free quantification of inflammation and characterization of inflammatory cellular and tissue alterations and related aspects of wound healing.

Evolution of treatment goals in IBD: from symptom control to histological healing

Core features of IBD pathophysiology comprise an impaired intestinal epithelial barrier function, commensal intestinal microbiota and a dysregulated intestinal immune system in genetically susceptible individuals (Wehkamp et al., 2016). IBD patients usually suffer from inflammation-associated symptoms such as abdominal pain, bloody diarrhea and fever. In addition, these symptoms are accompanied by a decreased quality of life (Baumgart and Sandborn, 2012, Ordas et al., 2012; Buono et al., 2017). Although the individual disease course is highly heterogeneous, the chronic inflammatory nature commonly results in significant intestinal damage over the long-term that is reflected by fistula and stricture development in CD patients and colitis-associated cancer development in UC patients (Solberg et al., 2007; Pariente et al., 2011; Baumgart and Sandborn, 2012; Peyrin-Biroulet et al., 2012; Bettenworth et al., 2016, Rieder et al., 2016, Hsu et al., 2017). Moreover, IBD represents a relevant entity in terms of socioeconomic costs given estimated average costs of $ 18963 for CD patients and $ 15020 for UC patients per year in the US (Park and Bass, 2011). Over recent years, uncontrolled intestinal inflammation has been recognized as the major driver for disease complications being associated with the need for surgery and high disease costs. Consequently, treatment goals for IBD patients have evolved targeting disease control: while symptom control was regarded as the primary treatment goal previously, more recent clinical trials have introduced the absence of endoscopic signs of mucosal inflammation, also referred to as mucosal healing, as primary endpoints due to the association with improved disease course (Froslie et al., 2007; Schnitzler et al., 2009; Colombel et al., 2011). More specifically, UC patients with absent mucosal inflammation were less likely to undergo colectomy (Froslie et al., 2007; Colombel et al., 2011), while CD patients with mucosal healing had prolonged clinical remission and reduced frequency of major surgery (Schnitzler et al., 2009).

Given the beneficial impact of mucosal healing in addition to symptom-control alone, it was hypothesized that complete histological resolution of inflammation (also referred to as *histological healing*) might be an even more powerful treatment goal (Villanacci et al., 2013). Indeed, there is a growing body of evidence demonstrating that mucosal healing may not necessarily be accompanied by histological healing and that persistent microscopic inflammation in UC patients is linked to more frequent relapses (Geboes and Dalle, 2002; Bessissow et al., 2012; Iacucci et al., 2015; Arijs et al., 2016; Kim et al., 2016a; Zenlea et al., 2016; Ozaki, 2017). The same association between ongoing histological disease activity and a worsened disease course was observed in CD patients (Dadalski, 2015). In line with the latter finding, a recent meta-analysis showed a strong correlation between persistent microscopic inflammation and a higher risk of colorectal neoplasia in UC patients (Colman and Rubin, 2016).

Common histological changes in UC patients include architectural distortion with crypt destruction, a predominantly mucosal inflammatory infiltrate and a basal plasmacytosis, whereas in CD discontinuous focal, chronic active mucosal inflammation with aphthous erosions often associated with underlying lymphoid aggregates, submucosal chronic inflammation disproportionate to that in the overlying mucosa and focal crypt irregularity are frequently found. Granulomas are uncommon and, if present, are poorly formed and associated with chronic inflammation in CD (Magro et al., 2013; Bryant et al., 2014). Several scoring systems to assess histological activity in UC and CD patients have been suggested and are summarized in Table 1 (Truelove and Richards, 1956; Matts, 1961; Watts et al., 1966; Korelitz and Sommers, 1974; Powell-Tuck et al., 1982; Keren et al., 1984; Friedman et al., 1986; Gomes et al., 1986; Saverymuttu et al., 1986; Floren et al., 1987; Riley et al., 1991; Hanauer et al., 1993; Odze et al., 1993; Sandborn et al., 1993; Nicholls et al., 1994; Breese et al., 1995; D'Haens et al., 1998; Geboes et al., 2000; D'Argenio et al., 2001; Fiel, 2003; Rutter et al., 2004; Feagan et al., 2005; Rubin, 2007; Laharie et al., 2011; Baars et al., 2012; Korelitz et al., 2014; Iacucci et al., 2015; Theede et al., 2015; Yarur et al., 2016; Jauregui-Amezaga et al., 2017; Marchal-Bressenot et al., 2017; Mosli et al., 2017a).

However, a uniform definition of histological remission does not yet exist for both UC and CD, and until now, no UC scoring system has been fully validated (Travis et al., 2011; Bryant et al., 2014; Mosli et al., 2014, 2017a,b). For UC, the most widely used scoring system is the Riley Index which evaluates acute inflammatory infiltrates, crypt abscesses, mucin depletion, breached surface epithelium, chronic inflammatory cell infiltrate and crypt architectural irregularities (Riley et al., 1991). The Geboes index evaluates similar features (neutrophils in the epithelium, lamina propria neutrophils and eosinophils, crypt

Table 1. Histological scoring systems for classification of inflammatory changes in IBD.

Score, year	Short scale description	Published studies	Validation level	Reference
Histological Scoring Systems in Ulcerative Colitis				
Truelove, 1956	Stepwise 3 grade scale: 1) no inflammation 2) mild to moderate inflammation 3) severe inflammation	Multiple clinical studies and RCT	Partially validated	Truelove and Richards, 1956
Matts, 1961	Stepwise 5 grade scale: 1) normal 2) some infiltration of the mucosa or lamina propria with either round cells or polymorphonuclear cells 3) much cellular infiltrate of the mucosa, lamina propria and submucosa 4) presence of crypt abscesses with much infiltration of all layers of the mucosa 5) ulceration, erosion, or necrosis of the mucosa with cellular infiltration of some or all of its layers	Multiple clinical studies and RCT	Not validated	Matts, 1961
Watts, 1966	Stepwise 4 grade scale: 0) normal 1) no significant epithelial changes but increased number of chronic inflammatory cells in the lamina propria 2) mild epithelial changes, usually regenerative, leukocytes may be seen in the crypts or ducts along with Paneth cells. Severe inflammatory cells can be seen in the lamina propria 3) severe inflammatory changes with evidence of crypt abscesses, inflammatory erosions and frank ulcerations	One clinical study	Not validated	Watts et al., 1966
Korelitz, 1974	Mucosal cell counting of rectal biopsies	Few clinical studies	Not validated	Korelitz and Sommers, 1974
Powell-Tuck, 1982	Stepwise 3 grade scale: 1) no inflammation 2) mild inflammation 3) moderate/severe inflammation	None	Not validated	Powell-Tuck et al., 1982
Keren, 1984	Dichotomic scale: inactive vs. active inflammation	None	Not validated	Keren et. al., 1984
Friedman, 1986	Stepwise 4 grade scale: 0) normal 1) lamina propria inflammation 2) crypt injury 3) ulceration	Multiple clinical studies and RCT	Not validated	Friedman et al., 1986
Saverymuttu, 1986	Stepwise grading system for 4 items: enterocyte damage, crypt abnormalities, lamina propria involvement and acute inflammatory infiltration in the lamina propria	Multiple clinical studies and RCT	Not validated	Saverymuttu et al., 1986
Gomes, 1986	Stepwise 5 grade scale: 0) normal 1) mild edema and inflammation in the lamina propria 2) crypt abscess formation and lamina propria involvement 3) destructive crypt abscesses with or without granulomas 4) active ulceration	Several clinical studies	Partially validated	Gomes et al., 1986
Floren, 1987	Stepwise 5 grade scale: 1) normal 2) slight inflammation 3) intermediate inflammation 4) severe inflammation 5) fulminant inflammation	Multiple clinical studies and RCT	Not validated	Floren et al., 1987
Riley, 1991	Stepwise 4 grade scale (none; mild; moderate; severe) for 6 items: acute inflammatory cell infiltrate, crypt abscesses, mucin depletion, surface epithelial integrity, chronic inflammatory cell infiltrate and crypt architectural irregularities	Multiple clinical studies and RCT	Partially validated	Riley et al., 1991
Hanauer, 1993	Stepwise 4 grade scale: normal colonic mucosa to high-grade active inflammation	Few clinical studies and RCT	Not validated	Hanauer et al., 1993
Odze, 1993	Stepwise 4 grade scale (normal; active; chronically active; chronically inactive) for 6 features: inflammation in lamina propria, crypt architectural abnormalities, lymphoid aggregates, basal plasmacytosis, viliform surface epithelial configuration and Paneth cell metaplasia	None	Not validated	Odze et al., 1993
Sandborn, 1993	Stepwise 4 grade scale: 0) inactive chronic colitis 1) mild active chronic colitis 2) moderately active chronic colitis 3) severely active chronic colitis	Few clinical studies and RCT	Not validated	Sandborn et al., 1993
Geboes, 2000	Stepwise grade scale for 7 items: architectural changes, chronic inflammatory infiltrates, lamina propria eosinophils, lamina propria neutrophils, epithelial neutrophils, crypt destruction, erosions or ulcerations	Few clinical studies and RCT	Most validated	Geboes et al., 2000
D'Argenio, 2001	Evaluation of 6 features: accumulation of lymphocytes and plasma cells, infiltration of neutrophils, crypt abscesses, ulceration, mucus depletion of epithelial cells and crypt distortion	Few clinical studies	Not validated	D'Argenio et al., 2001

Table 1. Continuation.

Harpaz, 2003	Stepwise 4 grade scale: a) inactive colitis b) mildly active colitis c) moderately active colitis d) severely active colitis	Few clinical studies	Partially validated	Fiel et al., 2003
Rutter, 2004	Stepwise 5 grade scale: 0) normal 1) quiescent/chronic inflammation 2) mild active inflammation 3) moderate active inflammation 4) severe active inflammation	None	Not validated	Rutter et al., 2004
Riley-Modification, 2005	Modification of former Riley score to better capture acute inflammatory changes	Few clinical studies	Partially validated	Feagan et al., 2005
Rubin, 2007	Stepwise 6 grade scale: 0) normal 1) quiescent 2) increased lamina propria granulocytes without definite intraepithelial granulocytes 3) intraepithelial granulocytes without crypt abscesses 4) crypt abscesses in less than 50 % of crypts 5) crypt abscesses in more than 50 % of crypts/erosion or ulceration	One clinical study	Partially validated	Rubin et al., 2007
Baars, 2012	Stepwise 4 grade scale: 0) no active disease 1) mild active inflammation 2) moderate active inflammation 3) severe active inflammation	None	Not validated	Baars et al., 2012
Korelitz, 2014	Stepwise 6 grade scale: degree of inflammation: 0) none 1) mild 2) moderate 3) severe 4) dysplasia 5) cancer	None	Not validated	Korelitz et al., 2014
Modified Harpaz-Score, 2015	Only slight modification of former Harpaz-Score	None	Partially validated	Theede et al., 2015
ECAP, 2015	ECAP-System: Extent of mucosal inflammation, Chronicity, Activity, Plus additional findings	Few clinical studies	Not validated	Iacucci et al., 2015
Yarur, 2016	Dichotomic scale: active or absent inflammation (defined as the presence/absence of inflammatory infiltrates [neutrophils in the lamina propria, basal plasmacytosis, basal lympoid aggregates])	None	Not validated	Yarur et al., 2017
Nancy Index, 2017	Stepwise 5 grade scale: 0) no/mild chronic inflammatory infiltrate (lymphocytes/plasmacytes) 1) moderate/marked chronic inflammatory infiltrate (lymphocytes/plasmacytes) 2) mild acute inflammatory cell infiltrate (neutrophils) 3) moderate to severe acute inflammatory cell infiltrate (neutrophils) 4) presence of ulceration	One clinical study	Most validated	Marchal-Bressenot et al., 2017
Robarts Index, 2017	Evaluation of 4 grades: chronic inflammatory infiltrate, lamina propria neutrophils, neutrophils in the epithelium and erosions/ulcerations	None	Most validated	Mosli et al., 2017a,b
Simplified Geboes, 2017	Simplification of the original Geboes score: concentrates only on items which are linked to active inflammation	None	Partially validated	Jauregui-Amezaga et al., 2017
Histological Scoring Systems in Crohn's Disease				
Nicholls, 1994	Stepwise 4 grade scale: 1) worse 2) no change 3) improvement 4) resolution of inflammation	None	Not validated	Nicholls et al., 1994
Breese, 1995	Evaluation of 5 items: ulceration, acute/chronic inflammation, crypt distorsion, goblet cell depletion and villous atrophy	None	Not validated	Breese et al., 1995
GHAS, 1998	Evaluation of 8 items: epithelial damage, architectural changes, mononuclear cells in lamina propria, neutrophils in lamina propria, erosion/ulceration, granuloma, number of segmental biopsy specimens affected	Few clinical trials	Not validated	D'Haens et al., 1998
Modified GHAS, 2011	Simplified: does not include the evaluation of the number of segmental biopsy specimens affected	One clinical trial	Not validated	Laharie et al., 2011
Baars, 2012	Stepwise 4 grade scale: 0) no active disease 1) mild active inflammation 2) moderate active inflammation 3) severe active inflammation	None	Not validated	Baars et al., 2012
Yarur, 2016	Dichotomic scale: active or absent inflammation (defined as the presence/absence of inflammatory infiltrates [neutrophils in the lamina propria, basal plasmacytosis, basal lymphoid aggregates])	None	Not validated	Yarur et al., 2017

Modified and extended from Mosli et al., 2014, Bryant et al., 2014 and Mosli et al., 2017b

destruction, erosion/ulceration and crypt destruction) and is, besides the recently developed Nancy- and the recently published Robarts-Index, the best validated scoring system for UC (Geboes et al., 2000; Jauregui-Amezaga et al., 2017; Marchal-Bressenot et al., 2017; Mosli et al., 2017a). For CD, several attempts have been conducted to establish scoring systems, but were hampered due to the discontinuous, transmural course of disease which impedes histological scoring (Bryant et al., 2014). Recently, the Colonic and Ileal Global Histology Disease Activity Scores (CGHAS/IGHAS) has been introduced (D'Haens et al., 1998; Laharie et al., 2011). This score reflects the extent of epithelial damage and architectural changes, the presence of mononuclear and polymorphonuclear cells in the lamina propria, polymorphonuclear cells in the epithelium, erosions or ulcers, granuloma and the number of affected biopsies.

A major drawback of nearly all currently available histological scoring systems is the lack of full validation and the missing integration of all pivotal aspects of IBD in most of the existing scoring systems such as basal plasmacytosis (Table 1) (Seldenrijk et al., 1991; Bryant et al., 2014; Mosli et al., 2014, 2017b). Additionally, accurate histological evaluation of IBD disease activity requires long-standing experience from a pathologist with gastrointestinal expertise (Mosli et al., 2014; Marchal et al., 2015).

Taken together, reliable, objective and easy-to-use systems for histological evaluation of disease activity in IBD patients are highly desirable and sophisticated techniques would essentially improve the quality of evaluation of histologic disease activity. Accurate and quantitative histological disease evaluation, ideal in a label-free manner, would contribute crucially to clinical decision making in order to achieve a better disease control, prevent the development of disabling complications and ultimately change the natural course of IBD.

Quantitative phase microscopy or label-free imaging of cells and tissue

Given the limitations of the currently available histological scoring systems for inflammatory bowel diseases we review and evaluate the capabilities of DHM as an example of QPI for histological quantification of intestinal inflammation and IBD-mediated tissue alterations and wound healing *in vitro*. QPI is based on the detection of optical path-length delay (OPD) that is induced by a mainly transparent unstained specimen against the surrounding environment (Fig. 1) (Kemper and von Bally, 2008; Kim, 2010; Popescu, 2011; Kemper et al., 2013; Lee et al., 2013; Marquet et al., 2014). In QPI, the illumination of the specimen is

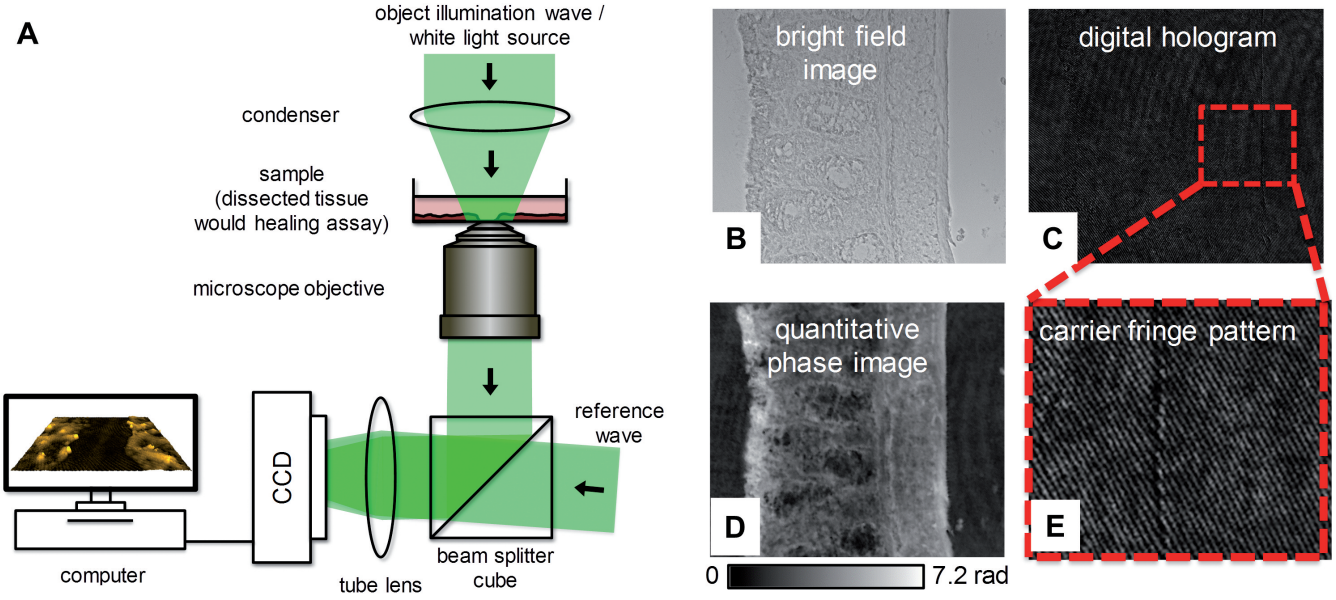

Fig. 1. Concept for quantitative phase imaging with digital holographic microscopy (DHM). **A.** A laser beam is divided into a reference and an object wave. Histological specimens like tissue slides or cell culture-based specimens such as *in vitro* wound healing assays induce optical path-length delays of the object against the surrounding medium which can be quantitatively assessed by recording the interference pattern of the superimposed object wave and the slightly tilted undisturbed reference wave utilizing a digital camera sensor, e. g. charge coupled device-(CCD)-sensor. **B, D.** Comparison of a standard bright field image and the corresponding numerically reconstructed quantitative DHM phase contrast image as an example of unstained healthy mouse colon sections, coded to 256 grey levels. **C.** Recorded digital off-axis hologram. **E.** The magnified insert of **(C)** illustrates the carrier fringe pattern in which the information about the optical path-length delay, caused by the object, is coded and from which the quantitative phase image in **(D)** can be calculated.

performed by transmission of light through the sample. Thus, only low intensities are required which minimize the interaction with the sample. During the past decade, various QPI techniques were developed and further improved for high resolution label-free quantitative *in vitro* live cell imaging as for example reported in (Cuche et al., 1999; Carl et al., 2004; Popescu et al., 2004, 2006; Ikeda et al., 2005; Mann et al., 2005; Marquet et al., 2005; Kemper et al., 2006, 2011; Choi et al., 2007; Kemper and von Bally, 2008; Bon et al., 2009; Debailleul et al., 2009; Kozacki et al., 2009; Shaked et al., 2009, 2010; Wang et al., 2011a,b; Shaked, 2012; Girshovitz and Shaked, 2013) and the analysis of unstained dissected tissues (Lue et al., 2007; Wang et al., 2011a; Lenz et al., 2013, 2016; Kemper, 2015). Recently, QPI microscopy technology has been made commercially available (www.lynceetec.com; www.phiab.se; www.tomocube.com; www.phasicscorp.com; www.phioptics.com; www.phasefocus.com; www.nanolive.ch) and also has been reported to be successfully modularly integrated into common optical microscopes (Kemper, 2006b; Bon et al., 2009; Shaked, 2012; Lee and Park, 2014) (www.phasicscorp.com; www.phioptics.com; www.phasefocus.com). Moreover, the compatibility of QPI for multimodal imaging in combination with other established imaging modalities such as bright field (Kemper et al., 2010b), fluorescence (Park et al., 2006, Kemper et al., 2010b; Pavillon et al., 2010; Esseling et al., 2012), confocal (Curl et al., 2005) or Raman microscopy (Kang et al., 2011; Pavillon et al., 2013) has been demonstrated. In various studies, different applications, for example, the analysis of blood cells (Park et al., 2009; Shaked et al., 2011; Chalut et al., 2012), endothelial cells (Seo, 2014), neuronal cells (Jourdain et al., 2011; Yang et al., 2017), cancer cell research (Kemper et al., 2006a; Kastl et al., 2017), apoptosis (Khmaladze, 2012), infection (Cho et al., 2012; Ekpenyong et al., 2013), sickle cell disease (Shaked et al., 2011; Jung et al., 2016), as well as usage in digital histopathology (Lue et al., 2007; Wang et al., 2011a,b; Lenz et al., 2013, 2016a,b; Kemper et al., 2015) and cell culture quality control (Kastl et al., 2017) were explored.

Laser holographic interferometric metrology is a well-established tool in industrial nondestructive testing and quality control (Kreis, 2006). In DHM, the reconstruction of digitally captured holograms is performed numerically (Kim, 2010). Thus, compared with state of the art Zernike phase microscopy (Zernike, 1955) and differential interference contrast (DIC) (Normaski, 1955), DHM offers quantitative phase contrast with optional subsequent numerical focus correction (multi-focus imaging) from single recorded holograms (Carl et al., 2004; Marquet et al., 2005). In contrast to fluorescence microscopy (Valeur, 2012) and label-free spectroscopic techniques like Fourier transform infrared (FTIR) spectroscopy (Movasaghi et al., 2008) or Raman spectroscopy (Rodriguez et al., 2006) that provide molecular specificity, DHM delivers global information that is related to cellular thickness and the spatial distribution of intracellular solute concentrations (Kemper, 2012; Kastl et al., 2017) and tissue density (Lue et al., 2007; Wang et al., 2011a, Lenz et al., 2013, 2016). In addition, DHM-based quantitative phase imaging requires only minimal sample preparation (Lenz et al., 2016), simplifies automated image segmentation (Mir et al., 2011; Kuhn et al., 2013; Bettenworth et al., 2014) and cell tracking (Langehanenberg et al., 2009; Kemper et al., 2010a; Memmolo et al., 2014) for quantification of cell morphology and motility, and allows the extraction of absolute biophysical parameter sets such as cellular volume, thickness and dry mass (Popescu et al., 2008; Rappaz et al., 2009; Mir et al., 2011; Bettenworth et al., 2014; Kastl et al., 2017). Finally, from quantitative DHM phase images the refractive index (RI) of the sample can be evaluated (Rappaz et al., 2005, 2008; Charriere et al., 2006; Choi et al., 2007, Kemper et al., 2007), which is directly related to cell and tissue functions and features including the cellular water content, intracellular solute concentrations (Liu et al., 2016) as well as tissue density (Lenz et al., 2013, 2016).

Quantification of inflammation degree utilizing the refractive index for label-free determination of tissue density

DHM has been evaluated in different settings in the context of infection and inflammation on a single cell level. For example, Yu et al. showed that DHM allowed monitoring of complex morphological changes of C6/36 cells during dengue virus infection. While the cell area and cell volume increased upon infection, the cell thickness of infected cells decreased in comparison to controls at several time points during a 24-hour period (Yu et al., 2017). Additionally, host cell interactions following bacterial infection with infectious pathogens have been studied by DHM. Ekpenyong and colleagues demonstrated a significantly reduced RI of primary murine bone marrow derived macrophages when stimulated with *Salmonella enterica serovar Typhimurium* (Ekpenyong et al., 2013). Park et al. tested QPI in the context of malaria detection (Park et al., 2008, 2016). Erythrocytes were infected by the malaria parasite *Plasmodium falciparum* and subsequently analyzed by QPI. Unstained erythrocytes were assessed for 23 morphological descriptors on available phase information in an automated algorithm-based manner: all individual morphological features differed significantly between infected and uninfected erythrocytes (Park et al., 2016). Another group evaluated quantitative phase spectroscopy for characterizing structural and biochemical changes of erythrocytes during the intraerythrocytic life cycle of *Plasmodium falciparum*. Due to analysis of changing amplitude and phase information, a 72.2% reduction of hemoglobin content as well as a 33.1% reduction of erythrocyte cell volume could be observed compared to uninfected cells

(Rinehart et al., 2016). Furthermore, the role of QPI in the life cycle of malaria was demonstrated by Chandamohanadas et al. when the authors observed *Plasmodium falciparum* infected erythrocytes shortly before rupturing and releasing matured schizonts. The use of protease inhibitors E64d and EGTA-AM to impede host-derived membrane rupture induced no cytoskeletal reconfiguration of erythrocytes which allowed the authors to analyze morphologic changes of schizonts prior to parasites' escape. Using tomographic phase microscopy, a significant change of the three-dimensional RI could be detected and additional analysis with diffraction phase microscopy revealed an elevated membrane fluctuation in inhibitor treated, infected erythrocytes (Chandramohanadas et al., 2011). Likewise, Diez-Silva et al. evaluated cellular changes of *Plasmodium falciparum* infected erythrocytes using diffraction phase microscopy and detected a *PF155/Ring-Infected Erythrocyte Surface Antigen* (*RESA*)-driven decrease of membrane fluctuation in infected erythrocytes in comparison to parasite-free controls (Diez-Silva et al., 2012).

Recently, we demonstrated QPI as assessed by DHM to be appropriate for automated quantification of inflammatory disease severity in the murine model of dextran sodium sulphate (DSS)-induced colitis (Fig. 2). More specifically, mice being treated with DSS for 6 days showed a moderate histological level of inflammation as assessed by the commonly used Dieleman score (Dieleman et al., 1998). The optical path-length delay (OPD) induced by stain-free colonic sections determined by DHM correlated well with the histological damage. Consequently, the RI, which is based on the OPD, was significantly decreased in all layers of the intestinal wall in colitic mice in comparison to healthy controls. Moreover, accurate differentiation between all layers of the intestinal wall based on DHM findings was feasible (Fig. 2) (Lenz et al., 2013). Given these promising results from experimental colitis models, colonic tissue samples from human CD patients were studied to evaluate the translational diagnostic potential of DHM (Fig. 3). Using the findings from endoscopic examinations and histological disease evaluation by Hematoxylin-Eosin-(HE)-staining as a gold standard, samples from CD patients with active flare of disease and in remission could be differentiated. Interestingly, significantly decreased RI values were observed in all layers of the intestinal wall in CD patients with active disease as compared to patients in remission (Lenz et al., 2016).

Label-free quantification of wound-healing *in vitro* by absolute biophysical parameters

There is growing evidence that DHM is appropriate for evaluation of cellular processes beyond infection and

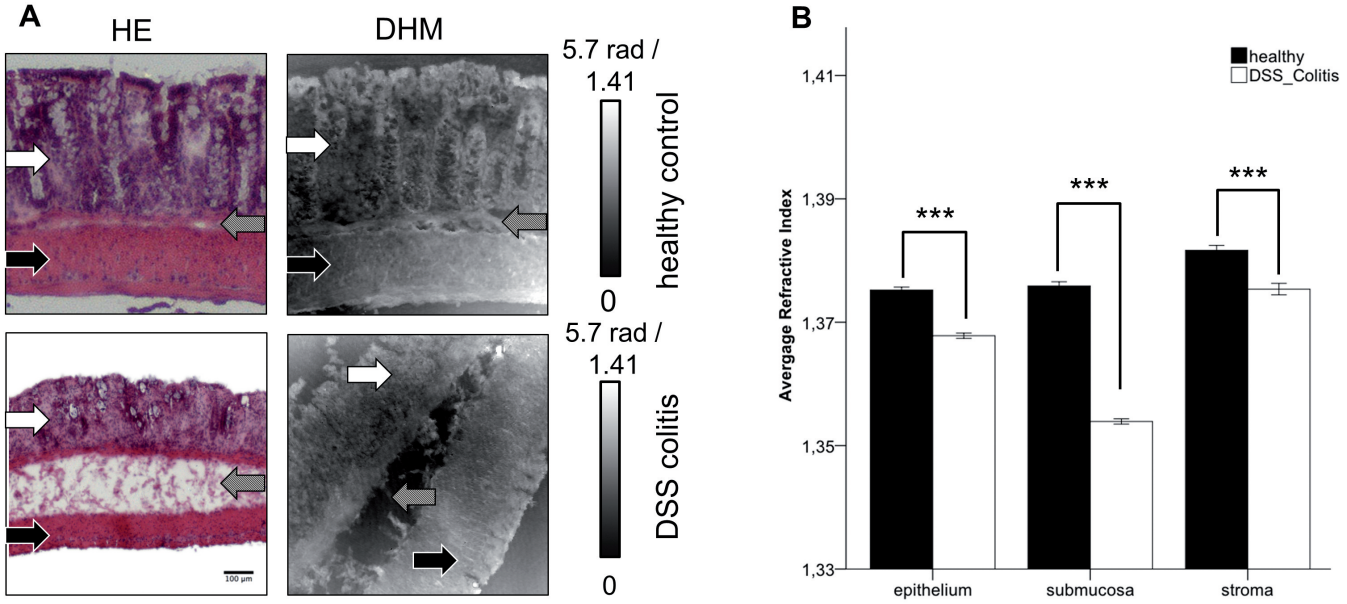

Fig. 2. DHM-based quantification of histological inflammation in a murine model of colitis. **A.** After induction of Dextran-sulfate-sodium-(DSS)-colitis in mice, histological evaluation was performed by conventional Hematoxylin-Eosin-(HE)-staining and DHM. Conventional histological analysis of HE-stained colonic tissue sections revealed marked mucosal inflammatory infiltrate, a submucosal edema and thickening of the muscularis propria. **B.** Evaluation of the corresponding DHM phase contrast images confirmed these changes and revealed significantly decreased refractive indices in all layers of the intestinal wall from colitic mice in comparison to healthy control animals (***p<0,001). Gray level bars indicate both detected optical path-length changes in radians, and the corresponding calculated refractive index values. Adapted from (Lenz et al., 2013, 2016).

inflammation (Ekpenyong et al., 2013; Lenz et al., 2013; Yu et al., 2017), and is therefore a promising approach to various other fields of cellular biology. Recently QPI was evaluated for classification of living healthy and cancerous cells using spatial morphological and textural information that was retrieved from label-free acquired QPI of cells. Using low-coherence interferometric phase microscopy, differences in 15 different biophysical parameters were analyzed, including OPD, dry mass, phase volume and surface area, which allowed Roitshtain and coworkers to differentiate healthy from primary tumor and metastatic cancer cells with a sensitivity of 81-93% and a specificity of 81-99% (Roitshtain et al., 2017). Molder et al. documented the long-term image-based impact of chemotherapeutic etoposide on the morphology of adherent living DU-145 cells. Low-dose treatment with etoposide resulted in a decreased proliferation rate of treated cells in comparison to untreated control cells as well as an increase in cell area and textural changes (Molder et al., 2017). Benzerdjeb et al. suggested DHM as a promising screening tool for cervical cancer, because DHM allowed differentiation of normal and abnormal cervical cells by reconstruction of 3-dimensional images and measurement of parameters like nuclear-to-cytoplasmic ratio and nuclear dimension (Benzerdjeb et al., 2016). DHM might also be helpful in elucidating immunological responses, as it was shown to be possible to discriminate between immune cell populations of CD4+ T-cells, B-cells and monocytes with average sensitivity rates of 92.2 to 97.5% and specificity rates of 86.4 to 95.1% (McReynolds et al., 2017). Confirming these results, DHM was able to discriminate CD4+/CD8+ T-cells and B-cells with an overall accuracy of 76% (Yoon, 2017). Interestingly, DHM was recently evaluated as a potential screening tool for diabetes. Using a single drop of blood, red blood cells (RBC) were obtained from diabetic and healthy patients and analyzed. The phase values of diabetic RBCs were significantly higher than those from healthy controls (Doblas et al., 2016). Another group evaluated morphological changes in erythrocytes of diabetic rats using phase-contrast digital holography. No changes between diabetic erythrocytes were observed in comparison to healthy controls when parameters such as perimeter, two-dimensional area, volume and three-dimensional surface were measured. However, a significant higher perimeter-to-area ratio as well as a significant lower surface area-to-volume ratio in diabetic erythrocytes was detected as compared to controls (Yeom et al., 2016). Employing three-dimensional quantitative phase imaging, Lee et al. analyzed erythrocytes of diabetic patients and reported that they could not detect any differences in morphological and biochemical parameters such as cell volume, surface area, sphericity, hemoglobin concentration and

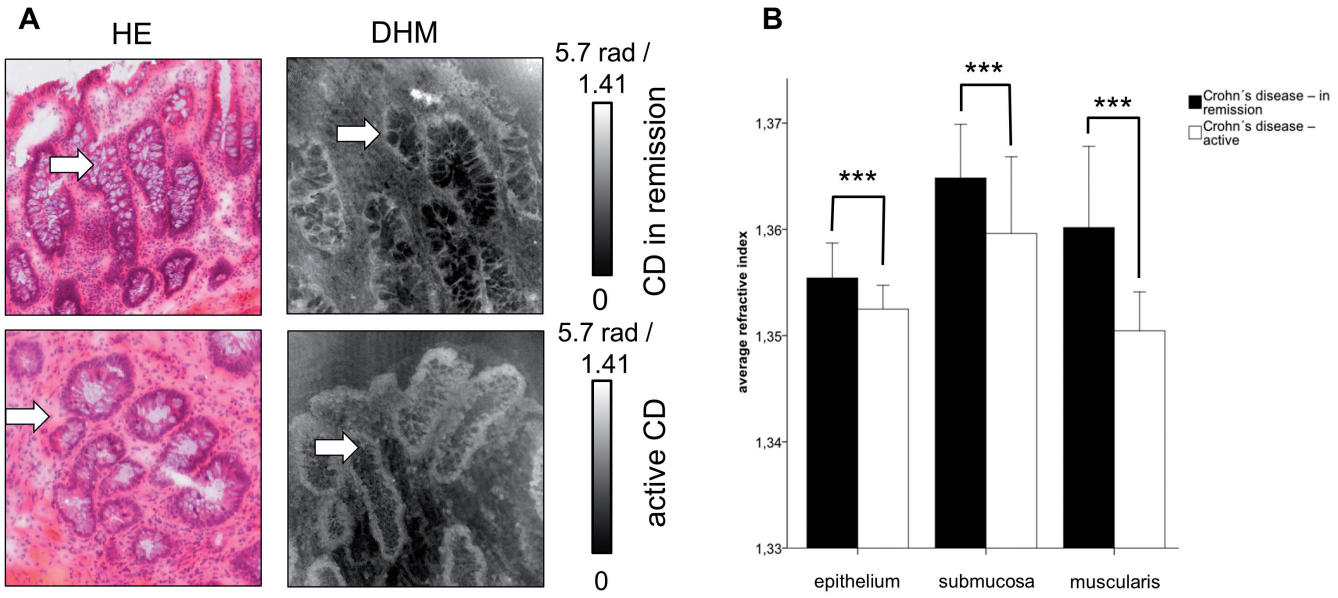

Fig. 3. DHM-based quantification of inflammation in colonic biopsies from Crohn's Disease patients. **A.** Colonic tissue samples from Crohn's disease patients in remission and CD patients with a flare of disease were assessed by conventional HE-staining and DHM. HE-staining revealed a pronounced inflammatory infiltrate, submucosal edema and a thickening of the muscularis propria. **B.** Corresponding DHM images confirmed these changes and determination of the refractive index revealed significant differences between biopsies from CD patients in remission and CD patients with a flare of disease in all layers of the intestinal wall (***p<0,001). Gray level bars indicate both detected optical path-length changes in radians, and the corresponding calculated refractive index values. Partly adapted from (Lenz et al., 2016).

hemoglobin content between diabetic erythrocytes in comparison to healthy controls but revealed a significantly lower membrane deformability of diabetic erythrocytes in comparison to controls (Lee et al., 2017).

Further to these proposed roles, DHM might also be important for non-invasive, stain-free monitoring of cell culturing. In L929 cells, Falck-Mionitis and colleagues analyzed changes of the cell phase volume upon chemically-induced cell cycle arrest, finding that G1-phase induced by staurosporine lead to a decreased average cell phase volume, while G2/M-phase cell cycle arrest stimulated with colcemid and etoposide induced an increase in average cell phase volume (Falck et al., 2014). In addition, DHM was evaluated for cell culture control: two pancreatic tumor cell lines were cultured at different confluence states and analyzed in cell culture media with varying osmolality; thereby changes of the cellular RI, cell radii volume and dry mass could be highly reliably determined (Kastl et al., 2017).

In the context of chronic inflammatory disorders, including IBD, wound healing represents an essential step during the resolution of inflammation. Therefore, we evaluated the potential usage of QPI to analyze wound closure of intestinal epithelial Caco-2 cells *in vitro* (Bettenworth et al., 2014, Lenz et al., 2016). Wound closure, comprising proliferation and migration of Caco-2 cells, was monitored by repetitive DHM-measurements (quantitative DHM phase images were acquired at least every 30 minutes for 40 hours) and additionally the effect of inhibiting and stimulating cytokine treatment was assessed. In addition to conventional monitoring of wound closure by white light microscopy, DHM was able to accurately follow the course of wound closure (Fig. 4). Moreover, considering the importance of altered morphological characteristics, DHM also provided continuous quantitative assessment of the temporal course of cellular volume, density, thickness, dry mass and cell number of Caco-2 cells that are accompanied by wound healing for the whole experimental period without the need for predefined specific end points (Figs. 5, 6). In addition, DHM could reliably quantify alterations of these features upon treatment with stimulating epidermal growth factor (EGF) and inhibiting mitomycin c: while the RI of EGF-treated Caco-2 cells was unchanged, the RI of mitomycin-treated cells was significantly reduced as compared to controls (Bettenworth et al., 2014). Furthermore cell covered surface area, average cell thickness, dry mass, cellular volume and total cell number of EGF-treated cells were significantly elevated

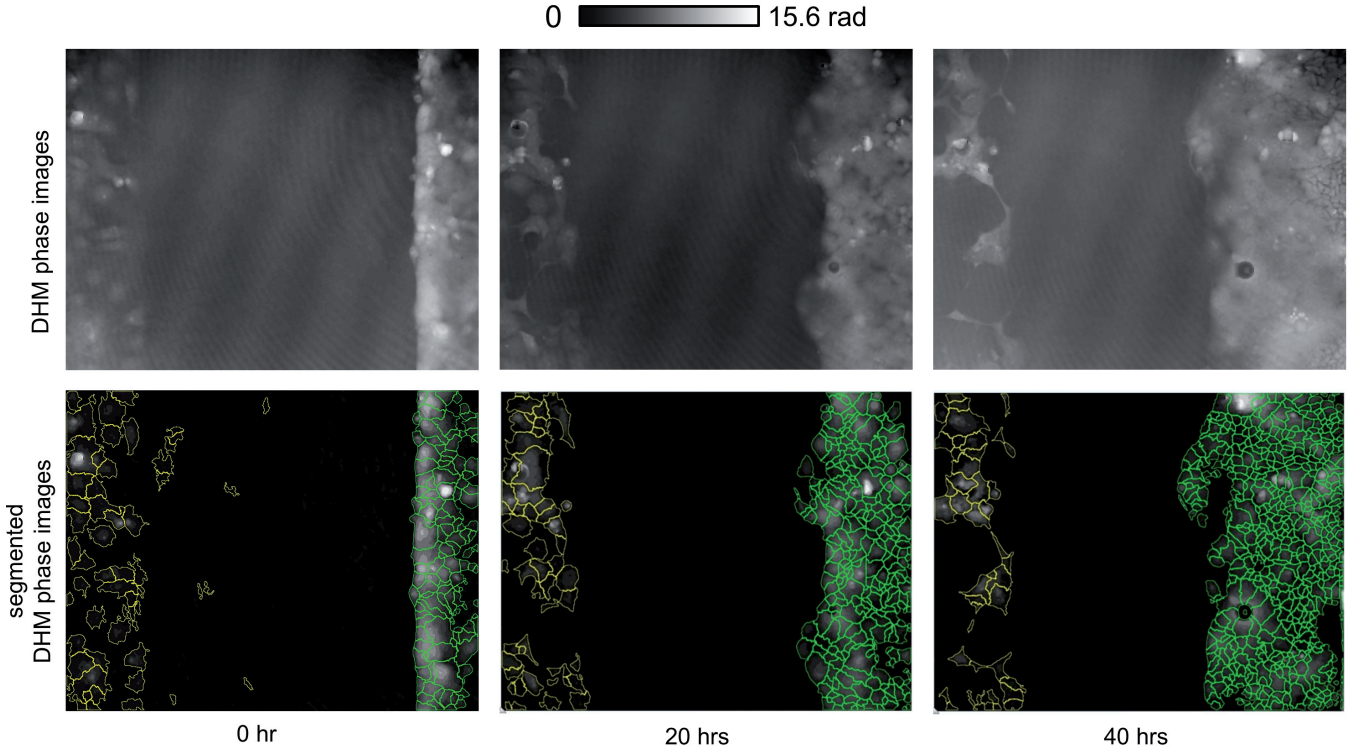

Fig. 4. Monitoring of epithelial wound healing *in vitro* by DHM. During *in vitro* wound healing assays with intestinal epithelial Caco-2-cells, DHM was reliably able to depict the outer border of cultured, unstained cell lines in a continuous manner (upper panel). In a subsequent analysis applying segmented DHM contrast images, cell outlines were displayed in an intensified way (lower panel). Adapted from (Bettenworth et al., 2014). The gray level bar indicates detected optical path-length changes in radians.

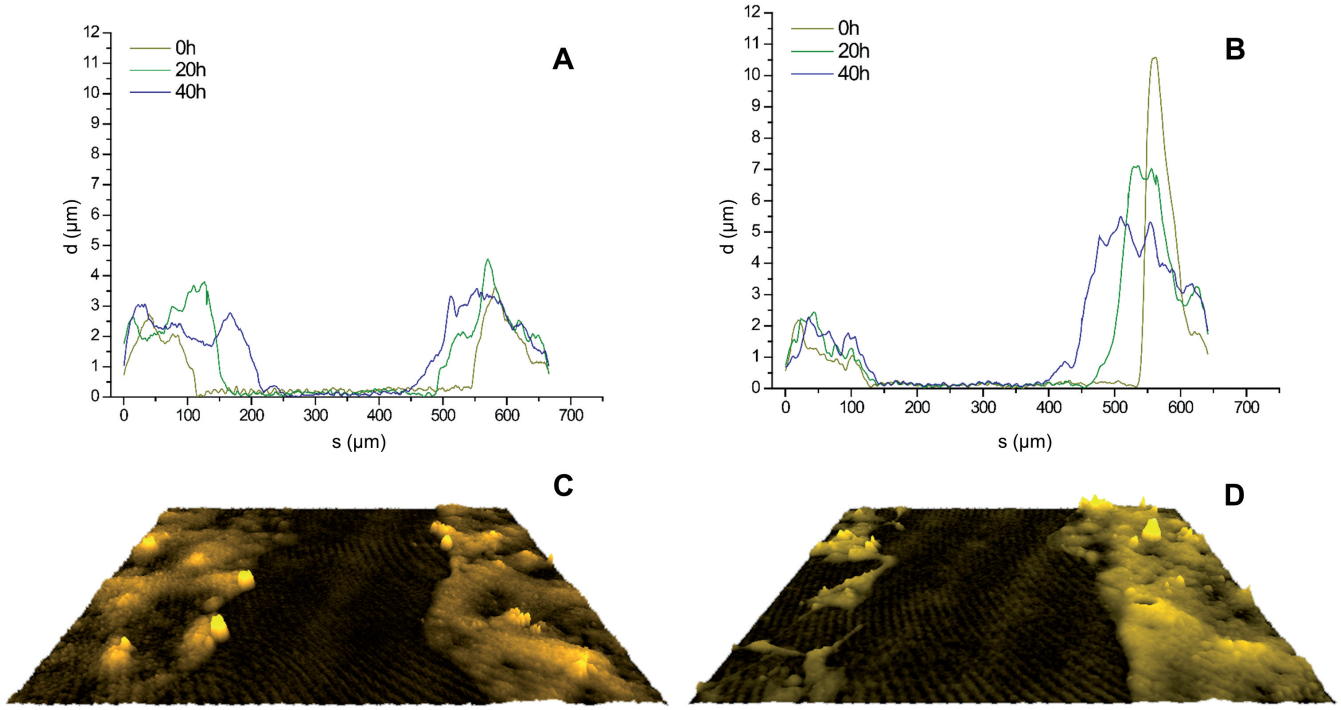

Fig. 5. Monitoring of the cellular thickness of epithelial cell layers during wound healing assays. **A.** Plots of the cellular thickness d (in μm) of intestinal epithelial Caco-2 cells in a wound healing assay and **(C)** the corresponding DHM image as a pseudo 3-D plot. **B, D.** Comparative wound healing assay of Caco-2 cells under stimulation with epidermal growth factor- (right) or mitomycin-c (left) shown as cell thickness profiles and corresponding illustration of cell morphology changes by DHM images as false color coded pseudo 3D plots. Adapted from (Bettenworth et al., 2014).

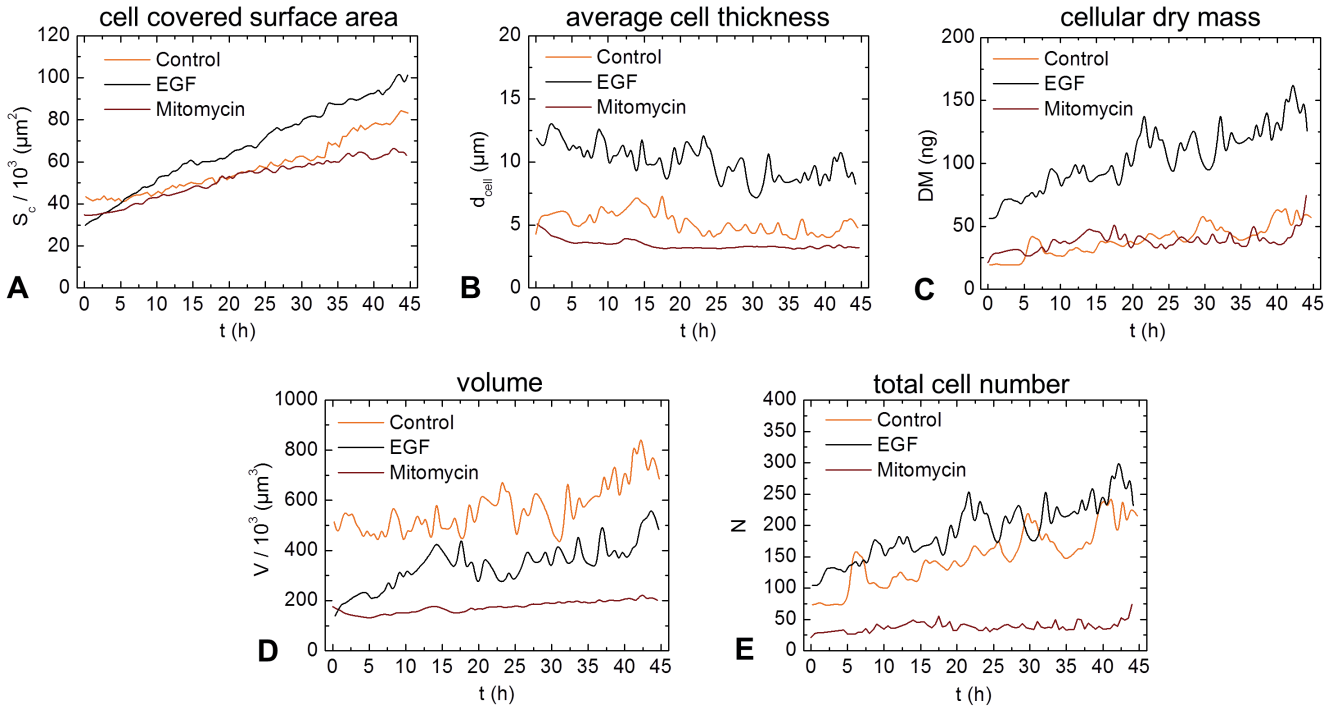

Fig. 6. Simultaneous continuous monitoring of cellular key characteristics in epithelial wound healing assays. In wound healing assays, epithelial Caco-2 cells were stimulated with either epidermal growth factor or mitomycin-c. Based on evaluation of quantitative phase image series from time-lapse investigation with DHM as illustrated in Fig. 4, the kinetics of the cell covered surface area **(A)**, the average cell thickness **(B)**, the accumulated cellular dry mass **(C)**, the cell volume **(D)** and the total cell number could be assessed in comparison to untreated control cells **(E)**. Adapted from (Lenz et al., 2016).

in comparison to mitomycin-c-treated cells (Fig. 6) (Lenz et al., 2016).

Limitations and outlook

Taken together, DHM as well as related quantitative imaging techniques have been demonstrated as powerful imaging tools and were evaluated for a wide spectrum of applications during the recent years. Based on the available data, QPI techniques such as DHM provide major advantages over other label-free light microscopy techniques such as bright field, Zernike and Nomarski differential phase contrast imaging modalities. The usage of QPI techniques can be significantly simplified by compact application matched with commercially available standalone systems (see providers of commercial QPI systems mentioned in section "Quantitative Phase Microscopy for label-free imaging of cells and tissue") or by modular integration of the technique into commonly used light microscopes, e. g. demonstrated for DHM in (Kemper, 2006; Lenz et al., 2016; Odenthal-Schnittler, 2016). The ability of QPI to quantitatively assess histological inflammation based on density changes in a stain-free and almost automated fashion appears especially to be appropriate for evaluation of histological damage in tissue samples from human IBD patients. Furthermore, the indication of DHM analysis may be further extended to dysplasia and malignancy detection and warrant further investigation in future studies.

Current restrictions of DHM concepts for imaging of dissected tissues and *in vitro* wound healing assays as sketched in Fig. 1 are some of the limitations of QPI image quality due to disturbances that are caused by the coherence properties of the applied laser light, the restricted specificity of QPI-based techniques as well as the lack of sufficient capabilities for 3D tomographic imaging of thicker tissues and cell layers. However, approaches have been reported to overcome several of these drawbacks and pave the way for sophisticated future developments. For example, the application of light sources with tailored coherence properties (Langehanenberg, 2010), modulation of the sample illumination (Choi et al., 2011; Schubert et al., 2014), and adapted multi-wavelength techniques (Kosmeier, 2012; Rinehart, 2012), have demonstrated an improvement in the signal-to-noise ratio of QPI significantly by reduction of coherence induced parasitic interference and scattering patterns. Moreover, it has been shown recently that multi-wavelength techniques provide label-free phase spectroscopy for hemoglobin concentration determination (Park et al., 2009) and thus promise the identification of specific cell types such as red blood cells by individual wavelength dependent refractive index signatures. Further enhancement for recognition of specific cell types and subcellular components can be expected by advanced image-processing procedures, polarization sensitive QPI and tomographic phase microscopy (TPM) approaches. For example, image processing based methods were shown to be capable of distinguishing between different types of blood cells (Shaked et al., 2011; Moon, 2012). Results reported by Aknoun et al. (2013) suggest that collagen fibers as well as their orientation inside cells can be imaged and identified by high-resolution polarization sensitive QPI-based retardance measurements. From recently reported findings obtained by TPM, it is evident that cells may be also recognized and distinguished by the three-dimensional refractive index distribution of their subcellular components in the future (Yoon et al., 2015; Habaza et al., 2017) and that cell layer thickness can be determined more accurately. Finally, a recently developed QPI-based selective technique, gradient light interference microscopy, enables imaging of tissue samples with dimensions in the range of only a several hundred micrometers (Nguyen et al., 2017).

Although already explored in some pilot studies (Kim et al., 2016b), a major remaining current future challenge is the still significantly limited capabilities for usage of DHM in *in vivo*-situations, as direct histological evaluation of colonic mucosa in IBD patients during endoscopy would be most desirable in the future.

In summary, DHM and related QPI techniques offer novel opportunities for enhanced quantitative assessment in IBD pathology and provide promising complementary biophysical information to existing histological evaluation and scoring systems as an objective, accurate and easy-to-use tool for assessing intestinal inflammation and are promising candidates to pave the way towards automated quantitative and label-free digital pathology.

References

Aknoun S., Bon P., Savatier J., Wattellier B. and Monneret S. (2013). Quantitative birefringence imaging of biological samples using quadri-wave interferometry. Proc. SPIE 8587, 85871D.

Arijs I., De Hertogh G., Lemmens B., Van Lommel L., de Bruyn M., Vanhove W., Cleynen I., Machiels K., Ferrante M., Schuit F., Van Assche G., Rutgeerts P. and Vermeire S. (2016). Effect of vedolizumab (anti-α4β7-integrin) therapy on histological healing and mucosal gene expression in patients with UC. Gut (in press).

Baars J.E., Nuij V.J., Oldenburg B., Kuipers E.J. and van der Woude C.J. (2012). Majority of patients with inflammatory bowel disease in clinical remission have mucosal inflammation. Inflamm. Bowel Dis. 18, 1634-1640.

Baumgart D.C. and Sandborn W.J. (2012). Crohn's disease. Lancet 380, 1590-1605.

Benzerdjeb N., Garbar C., Camparo P. and Sevestre H. (2016). Digital holographic microscopy as screening tool for cervical cancer preliminary study. Cancer Cytopathol. 124, 573-580.

Bessissow T., Lemmens B., Ferrante M., Bisschops R., Van Steen K., Geboes K., Van Assche G., Vermeire S., Rutgeerts P. and De Hertogh G. (2012). Prognostic value of serologic and histologic markers on clinical relapse in ulcerative colitis patients with mucosal healing. Am. J. Gastroenterol. 107, 1684-1692.

Bettenworth D., Lenz P., Krausewitz P., Bruckner M., Ketelhut S., Domagk D. and Kemper B. (2014). Quantitative stain-free and

continuous multimodal monitoring of wound healing *in vitro* with digital holographic microscopy. PloS One 9, e107317.

Bettenworth D., Nowacki T.M., Cordes F., Buerke B. and Lenze F. (2016). Assessment of stricturing crohn's disease: Current clinical practice and future avenues. World J. Gastroenterol. 22, 1008-1016.

Bon P., Maucort G., Wattellier B. and Monneret S. (2009). Quadriwave lateral shearing interferometry for quantitative phase microscopy of living cells. Opt. Express 17, 13080-13094.

Breese E.J., Michie C.A., Nicholls S.W., Williams C.B., Domizio P., Walker-Smith J.A. and MacDonald T.T. (1995). The effect of treatment on lymphokine-secreting cells in the intestinal mucosa of children with crohn's disease. Alimentary Pharmacol. Ther. 9, 547-552.

Bryant R.V., Winer S., Travis S.P. and Riddell R.H. (2014). Systematic review: Histological remission in inflammatory bowel disease. Is 'complete' remission the new treatment paradigm? An IOIBD initiative. J. Crohns Colitis 8, 1582-1597.

Buono J.L., Carson R.T. and Flores N.M. (2017). Health-related quality of life, work productivity, and indirect costs among patients with irritable bowel syndrome with diarrhea. Health Qual. Life Outcomes 15, 35.

Carl D., Kemper B., Wernicke G. and von Bally G. (2004). Parameter-optimized digital holographic microscope for high-resolution living-cell analysis. Appl. Opt. 43, 6536-6544.

Chalut K.J., Ekpenyong A.E., Clegg W.L., Melhuish I.C. and Guck J. (2012). Quantifying cellular differentiation by physical phenotype using digital holographic microscopy. Integr. Biol. (Camb), 280-284.

Chandramohanadas R., Park Y., Lui L., Li A., Quinn D., Liew K., Diez-Silva M., Sung Y., Dao M., Lim C.T., Preiser P.R. and Suresh S. (2011). Biophysics of malarial parasite exit from infected erythrocytes. PloS One 6, e20869.

Charriere F., Marian A., Montfort F., Kuehn J., Colomb T., Cuche E., Marquet P. and Depeursinge C. (2006). Cell refractive index tomography by digital holographic microscopy. Opt. Lett. 31, 178-180.

Cho S., Kim S., Kim Y. and Park Y. (2012). Optical imaging techniques for the study of malaria. Trends Biotechnol. 30, 71-79.

Choi W., Fang-Yen C., Badizadegan K., Oh S., Lue N., Dasari R.R. and Feld M.S. (2007). Tomographic phase microscopy. Nat. Methods 4, 717-719.

Choi Y., Yang, T.D., Lee, K.J. and Choi, W. (2011). Full-field and single-shot quantitative phase microscopy using dynamic speckle illumination. Opt. Lett. 36, 2465-2467.

Colman R.J. and Rubin D.T. (2016). Histological inflammation increases the risk of colorectal neoplasia in ulcerative colitis: A systematic review. Intest. Research 14, 202-210.

Colombel J.F., Rutgeerts P., Reinisch W., Esser D., Wang Y., Lang Y., Marano C.W., Strauss R., Oddens B.J., Feagan B.G., Hanauer S.B., Lichtenstein G.R., Present D., Sands B.E. and Sandborn W.J. (2011). Early mucosal healing with infliximab is associated with improved long-term clinical outcomes in ulcerative colitis. Gastroenterology 141, 1194-1201.

Cuche E., Marquet P. and Depeursinge C. (1999). Simultaneous amplitude-contrast and quantitative phase-contrast microscopy by numerical reconstruction of fresnel off-axis holograms. Appl. Opt. 38, 6994-7001.

Curl C.L., Bellair C.J., Harris T., Allman B.E., Harris P.J., Stewart A.G., Roberts A., Nugent K.A. and Delbridge L.M. (2005). Refractive index measurement in viable cells using quantitative phase-amplitude microscopy and confocal microscopy. Cytometry A 65, 88-92.

D'Argenio G., Cosenza V., Riegler G., Della Valle N., Deritis F., Mazzacca G. and Gruppo Italiano per lo Studio del Colon e del R. (2001). Serum transglutaminase correlates with endoscopic and histopathologic grading in patients with ulcerative colitis. Dig. Dis. Sci. 46, 649-657.

D'Haens G.R., Geboes K., Peeters M., Baert F., Penninckx F. and Rutgeerts P. (1998). Early lesions of recurrent crohn's disease caused by infusion of intestinal contents in excluded ileum. Gastroenterology 114, 262-267.

Dadalski. (2015). Histological improvement after induction therapy with infliximab provide prolonged clinical remission during maintenance therapy in children with crohn disease. EccO Congress 2015.

Debailleul M., Georges V., Simon B., Morin R. and Haeberle O. (2009). High-resolution three-dimensional tomographic diffractive microscopy of transparent inorganic and biological samples. Opt. Lett. 34, 79-81.

Dieleman L.A., Palmen M.J., Akol H., Bloemena E., Pena A.S., Meuwissen S.G. and Van Rees E.P. (1998). Chronic experimental colitis induced by dextran sulphate sodium (dss) is characterized by th1 and th2 cytokines. Clin. Exp. Immunol. 114, 385-391.

Diez-Silva M., Park Y., Huang S., Bow H., Mercereau-Puijalon O., Deplaine G., Lavazec C., Perrot S., Bonnefoy S., Feld M.S., Han J., Dao M. and Suresh S. (2012). Pf155/resa protein influences the dynamic microcirculatory behavior of ring-stage plasmodium falciparum infected red blood cells. Sci. Rep. 2, 614.

Doblas A., Roche E., Ampudia-Blasco F.J., Martinez-Corral M., Saavedra G. and Garcia-Sucerquia J. (2016). Diabetes screening by telecentric digital holographic microscopy. J. Microsc. 261, 285-290.

Ekpenyong A.E., Man S.M., Achouri S., Bryant C.E., Guck J. and Chalut K.J. (2013). Bacterial infection of macrophages induces decrease in refractive index. J. Biophotonics 6, 393-397.

Esseling M., Kemper B., Antkowiak M., Stevenson D.J., Chaudet L., Neil M.A., French P.W., von Bally G., Dholakia K. and Denz C. (2012). Multimodal biophotonic workstation for live cell analysis. J. Biophotonics 5, 9-13.

Falck Miniotis M., Mukwaya A. and Gjorloff Wingren A. (2014). Digital holographic microscopy for non-invasive monitoring of cell cycle arrest in l929 cells. PloS One 9, e106546.

Feagan B.G., Greenberg G.R., Wild G., Fedorak R.N., Pare P., McDonald J.W., Dube R., Cohen A., Steinhart A.H., Landau S., Aguzzi R.A., Fox I.H. and Vandervoort M.K. (2005). Treatment of ulcerative colitis with a humanized antibody to the alpha4beta7 integrin. N. Engl. J. Med. 352, 2499-2507.

Fiel M Q.L., Suriawinita A, Xu R, Qui L, Bitar M., Lee L. Harpaz N. (2003). Histologic grading of disease activity in chronic ibd: Inter- and intra-observer variation among pathologists with different levels of experience. Mod. Pathol. 16, 118A.

Floren C.H., Benoni C. and Willen R. (1987). Histologic and colonoscopic assessment of disease extension in ulcerative colitis. Scand. J. Gastroenterol. 22, 459-462.

Friedman L.S., Richter J.M., Kirkham S.E., DeMonaco H.J. and May R.J. (1986). 5-aminosalicylic acid enemas in refractory distal ulcerative colitis: A randomized, controlled trial. Am. J. Gastroenterol. 81, 412-418.

Froslie K.F., Jahnsen J., Moum B.A., Vatn M.H. and Group I. (2007). Mucosal healing in inflammatory bowel disease: Results from a norwegian population-based cohort. Gastroenterology 133, 412-422.

Geboes K. and Dalle I. (2002). Influence of treatment on morphological

features of mucosal inflammation. Gut 50 (Suppl 3), III 37-42.

Geboes K., Riddell R., Ost A., Jensfelt B., Persson T. and Lofberg R. (2000). A reproducible grading scale for histological assessment of inflammation in ulcerative colitis. Gut 47, 404-409.

Girshovitz P. and Shaked N.T. (2013). Compact and portable low-coherence interferometer with off-axis geometry for quantitative phase microscopy and nanoscopy. Opt. Express 21, 5701-5714.

Gomes P., du Boulay C., Smith C.L. and Holdstock G. (1986). Relationship between disease activity indices and colonoscopic findings in patients with colonic inflammatory bowel disease. Gut 27, 92-95.

Habaza M., Kirschbaum M., Guernth-Marschner C., Dardikman G., Barnea I., Korenstein R., Duschl C. and Shaked N.T. (2017). Rapid 3d refractive-index imaging of live cells in suspension without labeling using dielectrophoretic cell rotation. Advanced Science 4, 1600205.

Hanauer S., Schwartz J., Robinson M., Roufail W., Arora S., Cello J. and Safdi M. (1993). Mesalamine capsules for treatment of active ulcerative colitis: Results of a controlled trial. Pentasa study group. Am. J. Gastroenterol. 88, 1188-1197.

Hsu Y.C., Wu T.C., Lo Y.C. and Wang L.S. (2017). Gastrointestinal complications and extraintestinal manifestations of inflammatory bowel disease in taiwan: A population-based study. JCMA 56-62.

Iacucci M., Fort Gasia M., Hassan C., Panaccione R., Kaplan G.G., Ghosh S. and Gui X. (2015). Complete mucosal healing defined by endoscopic mayo subscore still demonstrates abnormalities by novel high definition colonoscopy and refined histological gradings. Endoscopy 47, 726-734.

Ikeda T., Popescu G., Dasari R.R. and Feld M.S. (2005). Hilbert phase microscopy for investigating fast dynamics in transparent systems. Opt. Lett. 30, 1165-1167.

Jauregui-Amezaga A., Geerits A., Das Y., Lemmens B., Sagaert X., Bessissow T., Lobaton T., Ferrante M., Van Assche G., Bisschops R., Geboes K., De Hertogh G. and Vermeire S. (2017). A simplified geboes score for ulcerative colitis. J. Crohns Colitis 11, 305-313.

Jourdain P., Pavillon N., Moratal C., Boss D., Rappaz B., Depeursinge C., Marquet P. and Magistretti P.J. (2011). Determination of transmembrane water fluxes in neurons elicited by glutamate ionotropic receptors and by the cotransporters kcc2 and nkcc1: A digital holographic microscopy study. J. Neurosci. 31, 11846-11854.

Jung J., Matemba L.E., Lee K., Kazyoba P.E., Yoon J., Massaga J.J., Kim K., Kim D.J. and Park Y. (2016). Optical characterization of red blood cells from individuals with sickle cell trait and disease in tanzania using quantitative phase imaging. Sci. Rep. 6, 31698.

Kang J.W., Lue N., Kong C.R., Barman I., Dingari N.C., Goldfless S.J., Niles J.C., Dasari R.R. and Feld M.S. (2011). Combined confocal raman and quantitative phase microscopy system for biomedical diagnosis. Biomed. Opt. Express 2, 2484-2492.

Kastl L., Isbach M., Dirksen D., Schnekenburger J. and Kemper B. (2017). Quantitative phase imaging for cell culture quality control. Cytometry A. 91, 470-481.

Kemper B. and von Bally G. (2008). Digital holographic microscopy for live cell applications and technical inspection. Appl. Opt. 47, A52-61.

Kemper B., Carl D., Schnekenburger J., Bredebusch I., Schafer M., Domschke W. and von Bally G. (2006a). Investigation of living pancreas tumor cells by digital holographic microscopy. J. Biomed. Opt. 11, 34005.

Kemper B., Carl, D., Höink A., von Bally G., Bredebusch I. and Schnekenburger J. (2006b). Modular digital holographic microscopy system for marker free quantitative phase contrast imaging of living cells. Proc. SPIE 6191.

Kemper B., Kosmeier S., Langehanenberg P., von Bally G., Bredebusch I., Domschke W. and Schnekenburger J. (2007). Integral refractive index determination of living suspension cells by multifocus digital holographic phase contrast microscopy. J. Biomed. Opt. 12, 054009.

Kemper B., Bauwens A., Vollmer A., Ketelhut S., Langehanenberg P., Muthing J., Karch H. and von Bally G. (2010a). Label-free quantitative cell division monitoring of endothelial cells by digital holographic microscopy. J. Biomed. Opt. 15, 036009.

Kemper B., Schmidt L., Przibilla S., Rommel C., Ketelhut S., Vollmer A., Schnekenburger J. and von Bally G. (2010b). Influence of sample preparation and identification of subcellular structures in quantitative holographic phase contrast microscopy. Proc. SPIE 7715.

Kemper B., Vollmer A., Rommel C.E., Schnekenburger J. and von Bally G. (2011). Simplified approach for quantitative digital holographic phase contrast imaging of living cells. J. Biomed. Opt. 16, 026014.

Kemper B., Klokkers J, Przibilla S., Vollmer A., Ketelhut S., von Bally G., Pavenstädt H.-J., Schlatter E. and Edemir, B. (2012). Tonicity induced changes in volume and refractive index of suspended cells quantified with digital holographic microscopy. Photonics Lett. Pol. 4, 45-47.

Kemper B., Langehanenberg P., Kosmeier S., Schlichthaber F., Remmersmann C., von Bally G., Rommel C., Dierker C. and Schneckenburg J. (2013). Digital holographic microscopy: Quantitative phase imaging and applications in live cell analysis. Handbook of Coherent-Domain Optical Methods pp 215-257.

Kemper B., Lenz P., Bettenworth D., Krausewitz P., Domagk D. and Ketelhut S. (2015). Influence of sample preparation and reliability of automated numerical refocusing in stain-free analysis of dissected tisues with quantitative phase digital holographic microscopy. International Society for Optics and Photonics 952904-952904-952906.

Keren D.F., Appelman H.D., Dobbins W.O. 3rd, Wells J.J., Whisenant B., Foley J., Dieterle R. and Geisinger K. (1984). Correlation of histopathologic evidence of disease activity with the presence of immunoglobulin-containing cells in the colons of patients with inflammatory bowel disease. Hum. Pathol. 15, 757-763.

Khmaladze R., Matz, R. L., Epstein, T., Jasensky, J., Banaszak Holl, M. M. and Chen, Z. (2012). Cell volume changes during apoptosis monitored in real time using digital holographic microscopy. J. Struct. Biol. 178, 270-278.

Kim M.K. (2010). Principles and techniques of digital holographic microscopy. J. Photonics Energy 018005-018005-018050.

Kim D.B., Lee K.M., Lee J.M., Chung Y.Y., Sung H.J., Paik C.N., Chung W.C., Jung J.H. and Choi H.J. (2016a). Correlation between histological activity and endoscopic, clinical, and serologic activities in patients with ulcerative colitis. Gastroenterol. Res. Pract. 2016, 5832051.

Kim K., Choe K., Park I., Kim P. and Park Y. (2016b). Holographic intravital microscopy for 2-d and 3-d imaging intact circulating blood cells in microcapillaries of live mice. Sci. Rep. 6, 33084.

Korelitz B.I. and Sommers S.C. (1974). Differential diagnosis of ulcerative and granulomatous colitis by sigmoidoscopy, rectal biopsy and cell counts of rectal mucosa. Am. J. Gastroenterol. 61, 460-469.

Korelitz B.I., Sultan K., Kothari M., Arapos L., Schneider J. and Panagopoulos G. (2014). Histological healing favors lower risk of colon carcinoma in extensive ulcerative colitis. World J. Gastroenterol. 20, 4980-4986.

Kosmeier S., Langehanenberg, P., von Bally, G. and Kemper, B. (2012). Reduction of parasitic interferences in digital holographic microscopy by numerically decreased coherence length. Appl. Phys. B 106, 107-115.

Kozacki T., Krajewski R. and Kujawinska M. (2009). Reconstruction of refractive-index distribution in off-axis digital holography optical diffraction tomographic system. Opt. Express 17, 13758-13767.

Kreis T. (2006). Handbook of holographic interferometry: Optical and digital methods. John Wiley & Sons.

Kuhn J., Shaffer E., Mena J., Breton B., Parent J., Rappaz B., Chambon M., Emery Y., Magistretti P., Depeursinge C., Marquet P. and Turcatti G. (2013). Label-free cytotoxicity screening assay by digital holographic microscopy. Assay Drug Dev. Technol. 11, 101-107.

Laharie D., Reffet A., Belleannee G., Chabrun E., Subtil C., Razaire S., Capdepont M. and de Ledinghen V. (2011). Mucosal healing with methotrexate in crohn's disease: A prospective comparative study with azathioprine and infliximab. Aliment. Pharmacol. Ther. 33, 714-721.

Langehanenberg P., Ivanova L., Bernhardt I., Ketelhut S., Vollmer A., Dirksen D., Georgiev G., von Bally G. and Kemper B. (2009). Automated three-dimensional tracking of living cells by digital holographic microscopy. J. Biomed. Opt. 14, 014018.

Langehanenberg P., von Bally G. and Kemper B. (2010). Appplication of partial coherent light in live cell imaging with digital holograpic microscopy. J. Mod. Opt. 57, 709-717.

Lee K. and Park Y. (2014). Quantitative phase imaging unit. Optics letters 39, 3630-3633.

Lee K., Kim K., Jung J., Heo J., Cho S., Lee S., Chang G., Jo Y., Park H. and Park Y. (2013). Quantitative phase imaging techniques for the study of cell pathophysiology: From principles to applications. Sensors 13, 4170-4191.

Lee M., Lee E., Jung J., Yu H., Kim K., Yoon J., Lee S., Jeong Y. and Park Y. (2016). Label-free optical quantification of structural alterations in alzheimer's disease. Sci. Rep. 6, 31034.

Lee S., Park H., Kim K., Sohn Y., Jang S. and Park Y. (2017). Refractive index tomograms and dynamic membrane fluctuations of red blood cells from patients with diabetes mellitus. Sci. Rep. 7, 1039.

Lenz P., Bettenworth D., Krausewitz P., Bruckner M., Ketelhut S., von Bally G., Domagk D. and Kemper B. (2013). Digital holographic microscopy quantifies the degree of inflammation in experimental colitis. Integr. Biol. (Camb) 5, 624-630.

Lenz P., Bruckner M., Ketelhut S., Heidemann J., Kemper B. and Bettenworth D. (2016). Multimodal quantitative phase imaging with digital holographic microscopy accurately assesses intestinal inflammation and epithelial wound healing. J. Vis. Exp. 115, e54460.

Liu P.Y., Chin L.K., Ser W., Chen H.F., Hsieh C.M., Lee C.H., Sung K.B., Ayi T.C., Yap P.H., Liedberg B., Wang K., Bourouina T. and Leprince-Wang Y. (2016). Cell refractive index for cell biology and disease diagnosis: Past, present and future. Lab. Chip 16, 634-644.

Lue N., Bewersdorf J., Lessard M.D., Badizadegan K., Dasari R.R., Feld M.S. and Popescu G. (2007). Tissue refractometry using hilbert phase microscopy. Opt. Lett. 32, 3522-3524.

Magro F., Langner C., Driessen A., Ensari A., Geboes K., Mantzaris G.J., Villanacci V., Becheanu G., Borralho Nunes P., Cathomas G., Fries W., Jouret-Mourin A., Mescoli C., de Petris G., Rubio C.A., Shepherd N.A., Vieth M., Eliakim R., European Society of P., European C.s. and Colitis O. (2013). European consensus on the histopathology of inflammatory bowel disease. J. Crohns Colitis 7, 827-851.

Mann C., Yu L., Lo C.M. and Kim M. (2005). High-resolution quantitative phase-contrast microscopy by digital holography. Opt. Express 13, 8693-8698.

Marchal Bressenot A., Riddell R.H., Boulagnon-Rombi C., Reinisch W., Danese S., Schreiber S. and Peyrin-Biroulet L. (2015). Review article: The histological assessment of disease activity in ulcerative colitis. Aliment. Pharmacol. Ther. 42, 957-967.

Marchal-Bressenot A., Salleron J., Boulagnon-Rombi C., Bastien C., Cahn V., Cadiot G., Diebold M.D., Danese S., Reinisch W., Schreiber S., Travis S. and Peyrin-Biroulet L. (2017). Development and validation of the nancy histological index for UC. Gut 66, 43-49.

Marquet P., Rappaz B., Magistretti P.J., Cuche E., Emery Y., Colomb T. and Depeursinge C. (2005). Digital holographic microscopy: A noninvasive contrast imaging technique allowing quantitative visualization of living cells with subwavelength axial accuracy. Opt. Lett. 30, 468-470.

Marquet P., Depeursinge C. and Magistretti P.J. (2014). Review of quantitative phase-digital holographic microscopy: Promising novel imaging technique to resolve neuronal network activity and identify cellular biomarkers of psychiatric disorders. Neurophotonics 1, 020901.

Matts S.G. (1961). The value of rectal biopsy in the diagnosis of ulcerative colitis. Q. J. Med. 30, 393-407.

McReynolds N., Cooke F.G., Chen M., Powis S.J. and Dholakia K. (2017). Multimodal discrimination of immune cells using a combination of raman spectroscopy and digital holographic microscopy. Sci. Rep. 7, 43631.

Memmolo P., Miccio L., Finizio A., Netti P.A. and Ferraro P. (2014). Holographic tracking of living cells by three-dimensional reconstructed complex wavefronts alignment. Opt. Lett. 39, 2759-2762.

Mir M., Wang Z., Shen Z., Bednarz M., Bashir R., Golding I., Prasanth S.G. and Popescu G. (2011). Optical measurement of cycle-dependent cell growth. Proc. Natl. Acad. Scie. USA 108, 13124-13129.

Molder A.L., Persson J., El-Schich Z., Czanner S. and Gjorloff-Wingren A. (2017). Supervised classification of etoposide-treated *in vitro* adherent cells based on noninvasive imaging morphology. J. Med. Imaging (Bellingham) 4, 021106.

Moon I., Javidi, B., Yi, F., Boss, D. and Marquet, P. (2012). Automated statistical quantification of three-dimensional morphology and mean corpuscular hemoglobin of multiple red blood cell. Opt. Express 20, 10295-10309.

Mosli M.H., Feagan B.G., Sandborn W.J., D'Haens G., Behling C., Kaplan K., Driman D.K., Shackelton L.M., Baker K.A., Macdonald J.K., Vandervoort M.K., Geboes K. and Levesque B.G. (2014). Histologic evaluation of ulcerative colitis: A systematic review of disease activity indices. Inflamm. Bowel Dis. 20, 564-575.

Mosli M.H., Feagan B.G., Zou G., Sandborn W.J., D'Haens G., Khanna R., Shackelton L.M., Walker C.W., Nelson S., Vandervoort M.K., Frisbie V., Samaan M.A., Jairath V., Driman D.K., Geboes K., Valasek M.A., Pai R.K., Lauwers G.Y., Riddell R., Stitt L.W. and Levesque B.G. (2017a). Development and validation of a histological index for uc. Gut 66, 50-58.

Mosli M.H., Parker C.E., Nelson S.A., Baker K.A., MacDonald J.K., Zou G.Y., Feagan B.G., Khanna R., Levesque B.G. and Jairath V. (2017b). Histologic scoring indices for evaluation of disease activity in ulcerative colitis. Cochrane Database Syst. Rev. 5, CD011256.

Movasaghi Z., Rehman, S. and Rehman D.I. (2008). Fourier transform infrared (ftir) spectroscopy of biological tissues. Appl. Spectrosc. Rev. 43, 134-139.

Nguyen T.H., Kandel M.E., Rubessa M., Wheeler M.B. and Popescu G. (2017). Gradient light interference microscopy for 3d imaging of unlabeled specimens. Nat. Commun. 8, 210.

Nicholls S., Domizio P., Williams C.B., Dawnay A., Braegger C.P., MacDonald T.T. and Walker-Smith J.A. (1994). Cyclosporin as initial treatment for crohn's disease. Arch. Dis. Child. 71, 243-247.

Normaski G. (1955). Differential microinterferometer with polarized waves. J. Phys. Radium 16, 9-11.

Odenthal-Schnittler M., Schnittler, H. J. and Kemper, B. (2016). Online quantitative phase imaging of vascular endothelial cells under fluid shear stress utilizing digital holographic microscopy Proc. SPIE 9718-97180U.

Odze R., Antonioli D., Peppercorn M. and Goldman H. (1993). Effect of topical 5-aminosalicylic acid (5-asa) therapy on rectal mucosal biopsy morphology in chronic ulcerative colitis. Am. J. Surg. Pathol. 17, 869-875.

Ordas I., Eckmann L., Talamini M., Baumgart D.C. and Sandborn W.J. (2012). Ulcerative colitis. Lancet 380, 1606-1619.

Ozaki. (2017). Histological risk factors to predict clinical relapse in ulcerative colitis in mucosal healing. ECCO Congress Barcelona 2017.

Pariente B., Cosnes J., Danese S., Sandborn W.J., Lewin M., Fletcher J.G., Chowers Y., D'Haens G., Feagan B.G., Hibi T., Hommes D.W., Irvine E.J., Kamm M.A., Loftus E.V., Jr., Louis E., Michetti P., Munkholm P., Oresland T., Panes J., Peyrin-Biroulet L., Reinisch W., Sands B.E., Schoelmerich J., Schreiber S., Tilg H., Travis S., van Assche G., Vecchi M., Mary J.Y., Colombel J.F. and Lemann M. (2011). Development of the crohn's disease digestive damage score, the lemann score. Inflamm. Bowel Dis. 17, 1415-1422.

Park K.T. and Bass D. (2011). Inflammatory bowel disease-attributable costs and cost-effective strategies in the united states: A review. Inflamm. Bowel Dis. 17, 1603-1609.

Park Y., Popescu G., Badizadegan K., Dasari R.R. and Feld M.S. (2006). Diffraction phase and fluorescence microscopy. Opt. Express 14, 8263-8268.

Park Y., Diez-Silva M., Popescu G., Lykotrafitis G., Choi W., Feld M.S. and Suresh S. (2008). Refractive index maps and membrane dynamics of human red blood cells parasitized by plasmodium falciparum. Proc. Natl. Acad. Scie. USA 105, 13730-13735.

Park Y., Yamauchi T., Choi W., Dasari R. and Feld M.S. (2009). Spectroscopic phase microscopy for quantifying hemoglobin concentrations in intact red blood cells. Opt. Lett. 34, 3668-3670.

Park H.S., Rinehart M.T., Walzer K.A., Chi J.T. and Wax A. (2016). Automated detection of p. Falciparum using machine learning algorithms with quantitative phase images of unstained cells. PloS One 11, e0163045.

Pavillon N., Benke A., Boss D., Moratal C., Kuhn J., Jourdain P., Depeursinge C., Magistretti P.J. and Marquet P. (2010). Cell morphology and intracellular ionic homeostasis explored with a multimodal approach combining epifluorescence and digital holographic microscopy. J. Biophotonics 3, 432-436.

Pavillon N., Hobro A.J. and Smith N.I. (2013). Cell optical density and molecular composition revealed by simultaneous multimodal label-free imaging. Biophys. J. 105, 1123-1132.

Peyrin-Biroulet L., Harmsen W.S., Tremaine W.J., Zinsmeister A.R., Sandborn W.J. and Loftus E.V. Jr (2012). Surgery in a population-based cohort of crohn's disease from olmsted county, minnesota (1970-2004). Am. J. Gastroenterol. 107, 1693-1701.

Popescu G. (2011). Quantitative phase imaging of cells and tissue. McGraw Hill Professional.

Popescu G., Deflores L.P., Vaughan J.C., Badizadegan K., Iwai H., Dasari R.R. and Feld M.S. (2004). Fourier phase microscopy for investigation of biological structures and dynamics. Opt. Lett. 29, 2503-2505.

Popescu G., Ikeda T., Dasari R.R. and Feld M.S. (2006). Diffraction phase microscopy for quantifying cell structure and dynamics. Opt. Lett. 31, 775-777.

Popescu G., Park Y., Choi W., Dasari R.R., Feld M.S. and Badizadegan K. (2008). Imaging red blood cell dynamics by quantitative phase microscopy. Blood Cells Mol. Dis. 41, 10-16.

Powell-Tuck J., Day D.W., Buckell N.A., Wadsworth J. and Lennard-Jones J.E. (1982). Correlations between defined sigmoidoscopic appearances and other measures of disease activity in ulcerative colitis. Dig. Dis. Sci. 27, 533-537.

Qiu Y., Chen B.L., Mao R., Zhang S.H., He Y., Zeng Z.R., Ben-Horin S. and Chen M.H. (2017). Systematic review with meta-analysis: Loss of response and requirement of anti-tnfalpha dose intensification in crohn's disease. J. Gastroenterol. 52, 535-554.

Rappaz B., Marquet P., Cuche E., Emery Y., Depeursinge C. and Magistretti P. (2005). Measurement of the integral refractive index and dynamic cell morphometry of living cells with digital holographic microscopy. Opt. Express 13, 9361-9373.

Rappaz B., Charriere F., Depeursinge C., Magistretti P.J. and Marquet P. (2008). Simultaneous cell morphometry and refractive index measurement with dual-wavelength digital holographic microscopy and dye-enhanced dispersion of perfusion medium. Opt. Lett. 33, 744-746.

Rappaz B., Cano E., Colomb T., Kuhn J., Depeursinge C., Simanis V., Magistretti P.J. and Marquet P. (2009). Noninvasive characterization of the fission yeast cell cycle by monitoring dry mass with digital holographic microscopy. J. Biomed. Opt. 14, 034049.

Rieder F., Latella G., Magro F., Yuksel E.S., Higgins P.D., Di Sabatino A., de Bruyn J.R., Rimola J., Brito J., Bettenworth D., van Assche G., Bemelman W., d'Hoore A., Pellino G. and Dignass A.U. (2016). European crohn's and colitis organisation topical review on prediction, diagnosis and management of fibrostenosing crohn's disease. J. Crohns Colitis 10, 873-885.

Riley S.A., Mani V., Goodman M.J., Dutt S. and Herd M.E. (1991). Microscopic activity in ulcerative colitis: What does it mean? Gut 32, 174-178.

Rinehart M., Zhu, Y. and Wax, A. (2012). Quantitative phase spectroscopy. Biomed. Opt. Express 3, 958-965.

Rinehart M.T., Park H.S., Walzer K.A., Chi J.T. and Wax A. (2016). Hemoglobin consumption by p. Falciparum in individual erythrocytes imaged via quantitative phase spectroscopy. Sci. Rep. 6, 24461.

Rodriguez L.G., Lockett S.J. and Holtom G.R. (2006). Coherent anti-stokes raman scattering microscopy: A biological review. Cytometry A 69, 779-791.

Roitshtain D., Wolbromsky L., Bal E., Greenspan H., Satterwhite L.L. and Shaked N.T. (2017). Quantitative phase microscopy spatial signatures of cancer cells. Cytometry A 91, 482-493.

Rubin D.T., Huo D., Hetzel J.T., Bunnag A.P., Sedrak M., Hart J.A. and Turner J.R. (2007). Increased degree of histological inflammation predicts colectomy and hospitalization in patients with ulcerative colitis. Gastroenterology 132:A19.

Rutter M., Saunders B., Wilkinson K., Rumbles S., Schofield G., Kamm M., Williams C., Price A., Talbot I. and Forbes A. (2004). Severity of inflammation is a risk factor for colorectal neoplasia in ulcerative colitis. Gastroenterology 126, 451-459.

Sandborn W.J., Tremaine W.J., Schroeder K.W., Steiner B.L., Batts K.P. and Lawson G.M. (1993). Cyclosporine enemas for treatment-resistant, mildly to moderately active, left-sided ulcerative colitis. Am. J. Gastroenterol. 88, 640-645.

Saverymuttu S.H., Camilleri M., Rees H., Lavender J.P., Hodgson H.J. and Chadwick V.S. (1986). Indium 111-granulocyte scanning in the assessment of disease extent and disease activity in inflammatory bowel disease. A comparison with colonoscopy, histology, and fecal indium 111-granulocyte excretion. Gastroenterology 90, 1121-1128.

Schnitzler F., Fidder H., Ferrante M., Noman M., Arijs I., Van Assche G., Hoffman I., Van Steen K., Vermeire S. and Rutgeerts P. (2009). Mucosal healing predicts long-term outcome of maintenance therapy with infliximab in crohn's disease. Inflamm. Bowel Dis. 15, 1295-1301.

Schubert R., Vollmer A., Ketelhut S. and Kemper B. (2014). Enhanced quantitative phase imaging in self-interference digital holographic microscopy using an electrically focus tunable lens. Biomed. Opt. Express 5, 4213-4222.

Seldenrijk C.A., Morson B.C., Meuwissen S.G., Schipper N.W., Lindeman J. and Meijer C.J. (1991). Histopathological evaluation of colonic mucosal biopsy specimens in chronic inflammatory bowel disease: Diagnostic implications. Gut 32, 1514-1520.

Seo W., Seo, E. and Lee, S.J. (2014). Cellular imaging using phase holographic microscopy: For the study of pathophysiology of red blood cells and human umbilical vein endothelial cells. J. Vis. (Tokyo) 17, 235-244.

Shaked N.T. (2012). Quantitative phase microscopy of biological samples using a portable interferometer. Opt. Lett. 37, 2016-2018.

Shaked N.T., Rinehart M.T. and Wax A. (2009). Dual-interference-channel quantitative-phase microscopy of live cell dynamics. Opt. Lett. 34, 767-769.

Shaked N.T., Zhu Y., Badie N., Bursac N. and Wax A. (2010). Reflective interferometric chamber for quantitative phase imaging of biological sample dynamics. J. Biomed. Opt. 15, 030503.

Shaked N.T., Satterwhite L.L., Telen M.J., Truskey G.A. and Wax A. (2011). Quantitative microscopy and nanoscopy of sickle red blood cells performed by wide field digital interferometry. J. Biomed. Opt. 16, 030506.

Solberg I.C., Vatn M.H., Hoie O., Stray N., Sauar J., Jahnsen J., Moum B., Lygren I. and Group I.S. (2007). Clinical course in crohn's disease: Results of a norwegian population-based ten-year follow-up study. Clin. Gastroenterol. Hepatol. 5, 1430-1438.

Theede K., Holck S., Ibsen P., Ladelund S., Nordgaard-Lassen I. and Nielsen A.M. (2015). Level of fecal calprotectin correlates with endoscopic and histologic inflammation and identifies patients with mucosal healing in ulcerative colitis. Clin. Gastroenterol. Hepatol. 13, 1929-1936.

Travis S.P., Higgins P.D., Orchard T., Van Der Woude C.J., Panaccione R., Bitton A., O'Morain C., Panes J., Sturm A., Reinisch W., Kamm M.A. and D'Haens G. (2011). Review article: Defining remission in ulcerative colitis. Aliment. Pharmacol. Ther. 34, 113-124.

Truelove S.C. and Richards W.C. (1956). Biopsy studies in ulcerative colitis. Br. Med. J. 1, 1315-1318.

Valeur B.B.-S., M.N. (2012). Molecular fluorescence: Principles and applications. John Wiley & Sons.

Villanacci V., Antonelli E., Geboes K., Casella G. and Bassotti G. (2013). Histological healing in inflammatory bowel disease: A still unfulfilled promise. World J. Gastroenterology 19, 968-978.

Wang Z., Tangella K., Balla A. and Popescu G. (2011a). Tissue refractive index as marker of disease. J. Biomed. Opt. 16, 116017.

Wang Z., Millet L., Mir M., Ding H., Unarunotai S., Rogers J., Gillette M.U. and Popescu G. (2011b). Spatial light interference microscopy (slim). Opt. Express 19, 1016-1026.

Watts J.M., Thompson H. and Goligher J.C. (1966). Sigmoidoscopy and cytology in the detection of microscopic disease of the rectal mucosa in ulcerative colitis. Gut 7, 288-294.

Wehkamp J., Gotz M., Herrlinger K., Steurer W. and Stange E.F. (2016). Inflammatory bowel disease. Dtsch Arztebl Int. 113, 72-82.

Yang S.A., Yoon J., Kim K. and Park Y. (2017). Measurements of morphological and biophysical alterations in individual neuron cells associated with early neurotoxic effects in parkinson's disease. Cytometry A. 91, 510-518.

Yarur A.J., Jain A., Hauenstein S.I., Quintero M.A., Barkin J.S., Deshpande A.R., Sussman D.A., Singh S. and Abreu M.T. (2016). Higher adalimumab levels are associated with histologic and endoscopic remission in patients with crohn's disease and ulcerative colitis. Inflamm. Bowel Dis. 22, 409-415.

Yeom E., Byeon H. and Lee S.J. (2016). Effect of diabetic duration on hemorheological properties and platelet aggregation in streptozotocin-induced diabetic rats. Sci. Rep. 6, 21913.

Yoon J., Kim K., Park H., Choi C., Jang S. and Park Y. (2015). Label-free characterization of white blood cells by measuring 3d refractive index maps. Biomed. Opt. Express 6, 3865-3875.

Yoon J., Jo, Y., Kim, M.-h., Kim, K., Lee, S., Kang, S.-J. and Park, Y. (2017). Label-free identification of non-activated lymphocytes using three-dimensional refractive index tomography and machine learning. bioRxiv.

Yu J.H., Liu X.L., Liu Y.J., He X.E., Hui Y., Zhang B., Zhu L. and Zhao W. (2017). Three-dimensional morphology of c6/36 cells infected by dengue virus: A study based on digital holographic microscopy. Nan Fang Yi Ke Da Xue Xue Bao 37, 301-307 (in chinesse).

Zenlea T., Yee E.U., Rosenberg L., Boyle M., Nanda K.S., Wolf J.L., Falchuk K.R., Cheifetz A.S., Goldsmith J.D. and Moss A.C. (2016). Histology grade is independently associated with relapse risk in patients with ulcerative colitis in clinical remission: A prospective study. Am. J. Gastroenterol. 111, 685-690.

Zernike F. (1955). How i discovered phase contrast. Science 121.

Accepted October 9, 2017